

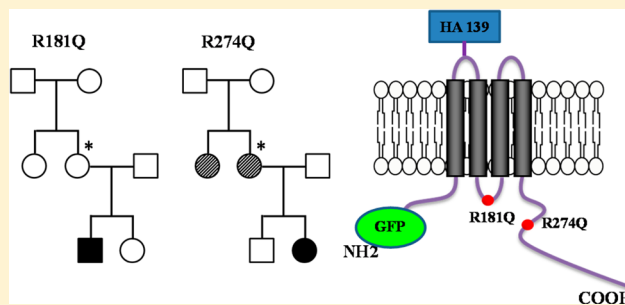
# Independent Mutations at Arg181 and Arg274 of Vangl Proteins That Are Associated with Neural Tube Defects in Humans Decrease Protein Stability and Impair Membrane Targeting

Alexandra Iliescu,<sup>†,‡</sup> Michel Gravel,<sup>†</sup> Cynthia Horth,<sup>†</sup> and Philippe Gros<sup>\*,†,‡</sup>

<sup>†</sup>Department of Biochemistry and <sup>‡</sup>Complex Traits Group, McGill University, Montreal, QC, Canada H3G-0B1

## S Supporting Information

**ABSTRACT:** In vertebrates, Vangl proteins play important roles during embryogenesis, including establishing planar polarity and coordinating convergent extension movements. In mice, homozygosity for mutations in the *Vangl1* and *Vangl2* genes or combined heterozygosity for *Vangl1/Vangl2* mutations causes the very severe neural tube defect (NTD) craniorachischisis. Recently, a number of patient-specific VANGL1 and VANGL2 protein mutations have been identified in familial and sporadic cases of mild and severe forms of NTDs. The biochemical nature of pathological effects in these mutations remains unknown. Of interest are two arginine residues, R181 and R274, that are highly conserved in Vangl protein homologues and found to be independently mutated in VANGL1 (R181Q and R274Q) and VANGL2 (R177H and R270H) in human cases of NTDs. The cellular and biochemical properties of R181Q and R274Q were established in transfected MDCK kidney epithelial cells and compared to those of wild-type (WT) Vangl1. Compared to that of WT, these mutations displayed impaired targeting to the plasma membrane and were instead detected in an intracellular endomembrane compartment that was positive for the endoplasmic reticulum. R181Q and R274Q showed impaired stability with significant reductions in measured half-lives from >20 h for WT protein to 9 and 5 h, respectively. These mutations have a cellular and biochemical phenotype that is indistinguishable from that of Vangl mutations known to cause craniorachischisis in mice (*Lp*). These results strongly suggest that R181 and R274 play critical roles in Vangl protein function and that their mutations cause neural tube defects in humans.



The neural tube is the primordial embryonic structure that gives rise to the brain and spinal cord. Failure of the neural tube to close properly results in neural tube defects (NTDs), a group of heterogeneous birth defects that are common in developed countries (0.5–2 per 1000 pregnancies).<sup>1–3</sup> Anencephaly, craniorachischisis, and myelomeningocele (spina bifida) represent the most severe forms of NTDs in which the neural tube remains partially or completely open.<sup>1</sup> The etiology of NTDs is complex and involves the interplay between genetic and environmental factors.<sup>4</sup> Population clustering, family (increased risk in siblings and first-degree relatives), and twin studies have established a genetic component to NTDs.<sup>1,5</sup> On the other hand, epidemiological studies have pointed at a strong environmental component in the etiology of NTDs: while hypothermia, diabetes, and psychological and emotional stress are associated with an increased risk of NTDs, perinatal folate supplementation has a strong protective effect.<sup>5</sup> Genetic mutations that cause NTDs in humans have been difficult to identify because of the polygenic nature of this heterogeneous trait, and the incomplete penetrance of genetic effects. However, the parallel characterization of mouse NTD mutants has provided a rich source of candidate genes whose relevance to human NTDs can be established in case control studies.<sup>6</sup>

In mice, positional cloning<sup>7,8</sup> and functional complementation studies<sup>9</sup> have shown that mutations in *Vangl2* cause the NTD phenotype in the *Loop-tail* (*Lp*) mutant. Homozygous *Lp/Lp* embryos die *in utero* and display craniorachischisis, a very severe NTD in which the neural tube remains completely open from hindbrain to the most caudal portion of the embryo. Individual loss-of-function *Vangl2* mutations have been identified in independent *Lp* mutant stocks, *Lp*(S464N), *Lp*<sup>m1/us</sup>(D255E), and *Lp*<sup>m2/us</sup>(R259L).<sup>7,10,11</sup> In vertebrates, there are two *Vangl* genes, *Vangl1* and *Vangl2*. The two encoded mRNAs and proteins are expressed during embryogenesis and show complementary expression patterns in the developing neural tube. *Vangl2* is expressed abundantly and broadly in the dorsal and ventral portions of the neural tube, prior to, during, and after closure (E7.5–E11.5), while *Vangl1* expression is mostly restricted to the ventral portion of the neural tube and to the notochord.<sup>7,12,13</sup> In addition, homozygosity for a loss-of-function *Vangl1* mutation<sup>13</sup> and double heterozygosity for *Vangl1*<sup>gt/+</sup>/*Vangl2*<sup>Lp/+13</sup> both give rise to craniorachischisis, suggesting a genetic interaction between

Received: April 2, 2014

Revised: June 23, 2014

Published: July 28, 2014

both genes, and further implicating both *Vangl1* and *Vangl2* as risk factors for NTDs. Finally, recent evidence suggests that *Vangl1* and *Vangl2* proteins may physically interact in certain cell types.<sup>14</sup>

*Vangl* proteins play a critical role in different aspects of cell and tissue patterning that has been conserved in evolution.<sup>4</sup> In flies, the *Vangl* homologue (*Van Gogh*; *Stbm*) provides positional cues and is required for polarization of certain epithelial layers and associated appendages.<sup>15,16</sup> This process is regulated by a set of planar cell polarity (PCP) genes that include *Vang*, *Frizzled* (*Fz*), *Dishevelled* (*Dvl*), *Prickle* (*Pk*), *Flamingo* (*Fmi*), and *Diego* (*Dgo*).<sup>17</sup> At the molecular level, PCP signaling in flies is associated with asymmetric positioning of membrane-bound *Dvl/Fz* and *Vang/Pk* complexes on opposite sides of adjacent cells, a distribution believed to propagate the polarity signal.<sup>18</sup> In vertebrates, the role of *Vangl* proteins in PCP signaling is preserved (e.g., polarization of ciliary bundles on sensory hair cells) and *Vangl* and other core PCP proteins (*Dvl*, *Fz*, and *Pk*) are required for convergent extension (CE) movements. This process, in which a group of cells intercalates in one direction and elongates in the perpendicular direction, fundamentally regulates many aspects of tissue patterning during embryogenesis, including neural tube closure, cardiogenesis, and the formation of various epithelial structures.<sup>19</sup> Mice bearing homozygous mutations in *Vangl2* or compound heterozygous for *Vangl2*<sup>Lp/+</sup> and other PCP gene mutations display multiple developmental defects, including craniorachischisis.<sup>4</sup>

*Vangl1* and *Vangl2* proteins are integral membrane proteins (521–526 amino acids) composed of four TM domains and a long C-terminal intracellular domain. The plasma membrane association of *Vangl* proteins has been verified in primary tissues *in vivo* and in transfected cultured cells *in vitro*,<sup>12,20,21</sup> and *Lp*-associated pathological mutations in mice cause a loss of *Vangl* membrane targeting.<sup>12,20,21</sup> The intracellular cytoplasmic domain of *Vangl* proteins contains a PDZ binding motif and interacts with other PCP proteins such as *Dvl* and *Sec24b*, and *Lp*-associated mutations (D255E and S464N) in the C-terminal domain impair these interactions.<sup>22,23</sup> The export of *Vangl* proteins from the trans-Golgi network (TGN) to the PM was also found to be mediated by the interaction between the Phe in the YXXF<sub>(280–283)</sub> motif and its binding with AP1, a clathrin adaptor complex.<sup>24</sup> Additionally, *Vangl2* has been shown to be phosphorylated in response to Wnt ligands, suggesting a possible regulation of *Vangl2*-dependent PCP signaling by morphogenic gradients.<sup>25,26</sup>

Mutations in *VANGL1* and *VANGL2*, all present in a heterozygous state, have been recently identified in human patients with NTDs. *VANGL1* mutations have been identified in a cohort of patients with sporadic (M328T) and familial (V239I and R274Q) cases of myelomeningocele (spina bifida).<sup>2</sup> Independently, mutations in human *VANGL2* (S84F, R353C, and F437S) were reported in stillborn fetuses with anencephaly and holoprosencephaly.<sup>27</sup> Complementation studies in zebrafish *trilobite* mutants (*Vangl* homologues) and protein–protein interaction assays have established that disease-associated *VANGL1* mutations V239I and M328T and *VANGL2* mutation F347S are functionally inactive.<sup>2,27</sup> Screening of additional cohorts of nonsyndromic sporadic cases of NTDs (cranial, open, and closed spinal dysraphisms) in patients from different ethnic origins identified 14 additional independent patient-specific *VANGL1* and *VANGL2* mutations.<sup>28–30</sup> In these studies, putative pathogenic mutations were

identified on the basis of (a) the absence of the mutation in ethnically matched controls, (b) evolutionary conservation of the affected residue, and (c) the nonconservative nature of the mutation. The possible effect of these mutations on *VANGL* protein function has yet to be determined. Of notable interest are two arginine residues at position 181 (R181) in the first intracellular loop linking TM2 and TM3 and at position 274 (R274) in the C-terminal intracellular half of the protein (*VANGL1* numbering). R181 is independently mutated (at the homologous position) to histidine in *VANGL2* (*VANGL2*<sup>R177H</sup>) and to glutamine in *VANGL1* (*VANGL1*<sup>R181Q</sup>) in two unrelated patients with NTDs. Likewise, R274 is independently mutated (at the homologous position) to histidine in *VANGL2* (*VANGL2*<sup>R270H</sup>) and to glutamine in *VANGL1* (*VANGL1*<sup>R274Q</sup>) in two unrelated patients with NTDs. R181 and R274 are extremely conserved in the *Vangl* protein family from flies to humans. Their independent mutations to nonconserved amino acids in independent patients with NTDs suggest not only that these mutations are pathological but also that R181 and R274 play a critical role in the function of the protein.

In this study, we have studied the function of R181 and R274 by characterizing the effects of mutations at these residues on the biochemical properties of the proteins.

## ■ EXPERIMENTAL PROCEDURES

**Material and Antibodies.** Restriction enzymes were obtained from New England Biolabs (Ipswich, MA), and Taq DNA polymerase was purchased from Invitrogen (Carlsbad, CA). The antibodies against the influenza hemagglutinin epitope (HA.11) (mouse monoclonal) and the c-Myc epitope (9e10) (mouse monoclonal) were purchased from Covance (Berkeley, CA). The antibody against Na,K-ATPase ( $\alpha$ 1 subunit) (mouse monoclonal) was purchased from Santa Cruz Biotechnology (Santa Cruz, CA). The antibody against calreticulin (rabbit polyclonal) was purchased from Affinity BioReagents (Golden, CO). Cy3-conjugated goat anti-mouse and anti-rabbit antibodies and the peroxidase-coupled goat anti-mouse antibody were from Jackson ImmunoResearch Laboratories (West Grove, PA). The reagents cycloheximide and MG-132 was purchased from Sigma-Aldrich (St. Louis, MO) and from Calbiochem (San Diego, CA), respectively. Geneticin (G418) and streptomycin were obtained from Invitrogen (Carlsbad, CA).

**Plasmids and Constructs.** Polymerase chain reaction overlap extension mutagenesis was used to introduce the R181Q, R274Q, and L202F mutations into the human *VANGL1* cDNA, as previously described.<sup>21</sup> All four constructs (*VANGL1*<sup>WT</sup>, *VANGL1*<sup>R181Q</sup>, *VANGL1*<sup>R274Q</sup>, and *VANGL1*<sup>L202F</sup>) contained a human c-Myc protein epitope tag (EQKLISEEDL) inserted at the N-terminus, a hemagglutinin (HA) epitope (YPYDVPDYA) inserted in the first extracellular loop at position 139 (used for cell surface detection and quantification of *VANGL1* protein expression), and green fluorescent protein (GFP) (used to facilitate detection of positive stable clones) at the N-terminus by cloning the various *VANGL1* cDNAs into a modified pGFP-C1 vector (Clontech, Mountain View, CA).

**Cell Culture and Transfection.** Madin-Darby canine kidney (MDCK) epithelial cells were maintained in Dulbecco's modified Eagle's medium (DMEM) supplemented with 10% fetal bovine serum (FBS), 100 units/mL penicillin, and 100  $\mu$ g/mL streptomycin at 37 °C in a 5% CO<sub>2</sub> incubator. MDCK cells were stably transfected with *VANGL1* constructs subcloned in pGFP-C1 using Lipofectamine Plus Reagent (Invitrogen) and

following the manufacturer's instructions. Stably transfected clones were selected in medium containing 0.4 mg/mL G418 for 10–14 days, and successful protein expression was identified by GFP fluorescence on live cells and confirmed by Western blotting analysis of cell extracts. Total cell lysates were prepared in RIPA buffer [50 mM Tris-HCl (pH 7.5), 150 mM NaCl, 5 mM EDTA, and 1% Triton X-100 supplemented with protease inhibitors], left on ice for 30 min, and spun down at 13000g for 10 min at 4 °C; 50 µg of protein from cell lysates was loaded onto 7.5% sodium dodecyl sulfate–polyacrylamide (SDS–PAGE) gels, followed by electroblotting and incubation with a monoclonal anti-HA antibody (HA.11) used at 1:1000 dilution, followed by incubation with a secondary horseradish peroxidase-conjugated goat anti-mouse antibody (1:5000), and visualization with enhanced chemiluminescence (SuperSignal West Femto Chemiluminescent Substrate Kit, Thermo Scientific, Rockford, IL).

**Quantification of Cell Surface Expression by an Enzyme-Linked Immunosorbent Assay.** Quantification of cell surface expression of HA-tagged Vangl1 (WT or mutant) proteins was performed using an enzyme-linked immunosorbent assay (ELISA) described previously<sup>21</sup> in which MDCK cells stably transfected with HA-tagged *VANGL1*<sup>WT</sup>, *VANGL1*<sup>R181Q</sup>, or *VANGL1*<sup>R274Q</sup> were grown to confluency in 24-well plates for 4 days. The cells were washed with PBS and incubated for 30 min in Ca<sup>2+</sup>-free DMEM, prior to incubation for 5 min with 10 mM EGTA. To quantify cell surface expression of HA-tagged Vangl1 proteins, cells were incubated with the mouse anti-HA antibody for 2 h (1:200 in Ca<sup>2+</sup>-free DMEM) (37 °C, 5% CO<sub>2</sub>), washed with PBS, fixed for 15 min with 4% paraformaldehyde in PBS, and incubated for 1 h with the HRP-conjugated goat anti-mouse antibody (1:4000 in a 5% nonfat milk/PBS mixture). To quantify total protein expression of HA-tagged Vangl1 proteins, cells were fixed immediately after the EGTA treatment, permeabilized for 30 min with 0.1% Triton X-100 in PBS, blocked for 30 min in a 5% nonfat milk/PBS mixture, incubated with the anti-HA antibody (1:200 in blocking solution) for 1 h, washed with PBS, and incubated with the HRP-conjugated goat anti-mouse antibody (1:4000 in blocking solution). Both cell surface expression and total cell expression were quantified colorimetrically using the HRP substrate [0.4 mg/mL *O*-phenylenediamine dihydrochloride (OPD) (Sigma-Aldrich)] according to the manufacturer's instructions. The reaction was stopped via addition of 3 N HCl; absorbance readings (492 nm) were taken in an ELISA plate reader, and the background absorbance reading from the nonspecific binding of the primary antibody to vector-transfected cells was subtracted for each sample. Cell surface readings were normalized to the total HA-tagged GFP-*VANGL1* value for each cell clone and are expressed as a percentage.

**Metabolic Labeling, Pulse–Chase Study, and Immunoprecipitation.** MDCK cells stably expressing Vangl1<sup>WT</sup>, Vangl1<sup>R181Q</sup>, or Vangl1<sup>R274Q</sup> proteins were grown to confluency for 48 h in 60 mm plastic dishes. Cells were then incubated for 90 min at 37 °C in methionine- and cysteine-free DMEM containing 10% dialyzed FBS (labeling medium). This was followed by a 60 min incubation at 37 °C with 2 mL of labeling medium containing 100 µCi of [<sup>35</sup>S]methionine-cysteine (PerkinElmer, Boston, MA). Cells were washed twice with PBS and incubated for different periods of time (up to 16 h) in 2 mL of chase medium (standard DMEM containing 10% FBS, 15 µg/mL methionine, and 15 µg/mL cysteine). Total cell

lysates were prepared in 400 µL of RIPA buffer, and equal amounts of cell lysates were subjected to immunoprecipitation using mouse anti-cMyc antibody 9E10 (2.5 µg) in RIPA buffer and incubated overnight at 4 °C. The following day, proteins were incubated for 4 h at 4 °C with protein A/G-Sepharose (GE Healthcare, Piscataway, NJ), followed by three washes in RIPA buffer, and eluted with 50 µL of 3× sample buffer. Radiolabeled proteins were separated by electrophoresis on 7.5% SDS–PAGE gels. Gels were fixed for 30 min in a 40% MeOH/10% acetic acid mixture, soaked for 15–30 min in Amplify (GE Healthcare), dried, and exposed to film. Band intensity was quantified using ImageJ (National Institutes of Health, Bethesda, MD).

**Determination of Relative Protein Stability.** To determine the stability of wild-type and mutant Vangl1 protein mutations, MDCK cells stably expressing these proteins were grown to confluency (48 h) and treated for 6 h with cycloheximide (20 µg/mL) in the presence or absence of MG-132 (5 µg/mL). Total cell lysates were prepared with RIPA buffer, and 50 µg of protein was loaded on a 7.5% SDS–PAGE gel, followed by immunoblot analysis using the anti-HA antibody. Band intensities of Western blot gels were quantified using data from three independent experiments and quantitated using ImageJ, with β-actin used as an internal loading control.

**Immunofluorescence and Confocal Microscopy.** MDCK cells stably expressing different Vangl1 proteins were examined for protein expression under both permeabilized (total cell expression) and nonpermeabilized conditions (cell surface expression), and at confluency on glass coverslips in a 12-well plate. Cells were washed twice with PBS, fixed for 15 min in 4% PFA in PBS, permeabilized with 0.5% Triton X-100 in PBS for 15 min, blocked in 5% goat serum in PBS for 1 h, incubated with the desired primary antibody [mouse anti-Na,K-ATPase (1:100), mouse anti-HA (1:200), and rabbit anti-calreticulin (1:100)] for 1 h, and washed three times with 0.1% BSA in PBS. Finally, the coverslips were incubated for 1 h with the appropriate secondary antibody [goat anti-mouse-Cy3 (1:1000) and goat anti-rabbit-Cy3 (1:1000)] and washed three times with 0.1% BSA in PBS. All the incubations were conducted at room temperature, and the antibodies were all diluted in a blocking solution. To detect cell surface expression of the exofacial HA epitope engineered in Vangl1 proteins (nonpermeabilized conditions), MDCK cells expressing GFP-Vangl1 WT, R181Q, or R274Q were incubated with the mouse anti-HA antibody (1:200) in DMEM containing 2% nonfat milk for 2 h at 37 °C. After being washed several times with PBS, cells were fixed for 15 min with 4% PFA in PBS and incubated with the goat anti-mouse-Cy3 antibody (1:1000) for 1 h. For immunofluorescence, coverslips were rinsed once in water and mounted with Permafluor Aqueous Mounting Medium (Thermo Scientific, Fremont, CA). Confocal microscopy was performed using a Zeiss LSM5 Pascal laser scanning confocal microscope. All image analyses were performed using the LSM5 Image software.

## RESULTS

**R181Q and R274Q Mutations Associated with Human Neural Tube Defects.** More than 20 human *VANGL1* and *VANGL2* mutations have been found to be associated with human neural tube defects (NTDs).<sup>2,27–30</sup> The mechanistic basis for the loss of VANGL protein function in these human disease-associated mutations has not been studied. Two arginine residues at positions 181 (R181) and 274 (R274)



(*VANGL1* nomenclature) attracted our attention for several reasons. First, R181 and R274 are independently mutated (a) to glutamine in *VANGL1* (R181Q and R274Q) in two unrelated NTD patients and (b) to histidine in *VANGL2* (R177H and R270H) at the homologous position in two other unrelated NTD patients. Second, both R181 and R274 are extremely conserved in the *VANGL* family, R274 being invariant and R181 being highly conserved, with both mapping to protein subdomains that also show a high degree of sequence conservation among family homologues and orthologs (Figure 1). Finally, the charged positive side chain of arginine is lost in

*VANGL2* mutations (R173H and R186H) associated with NTDs in an Eastern European cohort.<sup>30</sup>

Together, these results suggest that R181 and R274 play important and evolutionarily conserved structural or functional roles in the Vangl protein family and suggest that loss of either arginine (in independent NTD patients) is detrimental to function, ultimately leading to NTDs. Therefore, we have studied the potential molecular defect in the R181Q and R274Q mutants following their reconstruction in a human *VANGL1* backbone and expression in transfected cells.

#### Expression and Cellular Localization of R181Q and R274Q *VANGL1* Mutations in Stably Transfected MDCK Cells.

Targeting of Vangl proteins to the plasma membrane is essential for biological function and PCP signaling. In mouse embryos, the Vangl2 protein is targeted to the basolateral membrane of several epithelial cells and tubular structures. *Lp* mouse mutant embryos with craniorachischisis show a reduced level of Vangl2 protein expression and loss of membrane targeting.<sup>12</sup> To investigate the effect of the R181Q and R274Q mutations on the biochemical properties of Vangl proteins, the two mutations were expressed as GFP fusion proteins in MDCK cells. This cell type was chosen because it is derived from a lineage (kidney tubules) that normally expresses Vangl proteins and is likely to possess the cellular machinery required for the proper expression, maturation, and subcellular targeting of the protein. We have previously shown that WT Vangl1 protein is targeted to the basolateral membrane of MDCK cells and that this membrane targeting is lost in *Lp*-associated Vangl2 protein mutations (D255E, R259L, and S464N) that cause craniorachischisis in mice.<sup>20,21</sup>

MDCK cells were transfected with plasmids (see Experimental Procedures) expressing either WT or mutant Vangl1 mutations R181Q and R274Q (as GFP- and HA-tagged fusions), followed by the isolation of single clones stably expressing each protein. These were initially selected by epifluorescence (GFP positive), followed by immunoblotting of crude membrane extracts (data not shown) with an anti-HA antibody directed against an exofacial HA epitope tag inserted in the extracellular domain defined by the TM1–TM2 interval (Figure 1). A possible effect of the R181Q and R274Q mutations on plasma membrane targeting of the protein was then investigated in these clones by double immunofluorescence. WT Vangl1 shows strong expression at the plasma membrane: it produces a typical “meshlike” staining pattern that shows strong colocalization with the plasma membrane marker Na,K-ATPase (Figure 2A, top panel). On the other hand, R181Q and R274Q do not appear to be concentrated at the plasma membrane but rather show a diffuse cytoplasmic signal and do not colocalize with Na,K-ATPase (Figure 2A, middle and bottom panels), suggesting that both mutations alter the normal targeting of Vangl1 to the plasma membrane. Normal plasma membrane targeting of Vangl1 in MDCK cells results in exposure of the TM1–TM2 domain of the protein to the extracellular milieu, where it can be recognized by antibodies directed against an HA epitope tag inserted at that site.<sup>21</sup> The polarity and degree of exposure of this exofacial HA to the extracellular milieu were monitored in WT-, R181Q-, and R274Q-expressing cells by immunofluorescence with an anti-HA antibody in intact cells versus cells permeabilized with 0.5% Triton X-100. Results in Figure 2B (top panel) show that the WT Vangl1 protein is detected in both intact and permeabilized cells, where it shows punctate cell surface staining (permeabilized). By contrast, R181Q and R274Q

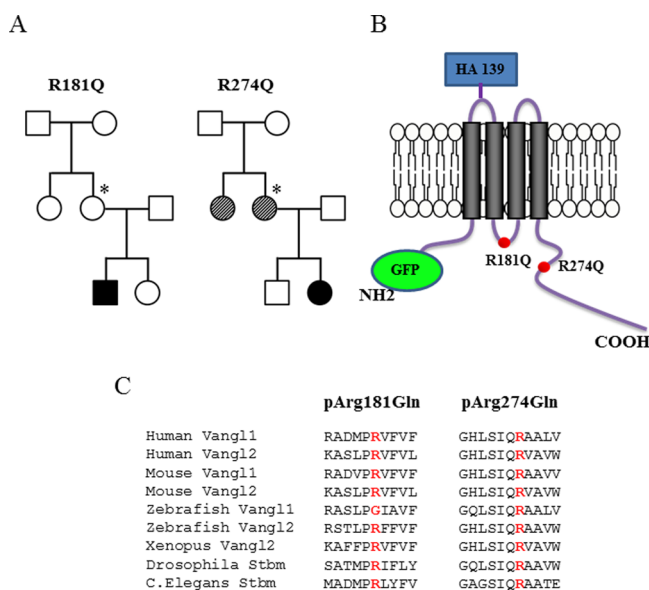


**Figure 1.** Pedigree and schematic representation of human mutations (R181Q and R274Q) found in NTD patients. (A) Familial pedigree showing the R181Q mutation in a patient with myelomeningocele, a mutation also present in the mother (asterisk) but absent in the father and unaffected sister, a case with a positive familial history of myelomeningocele in a distant maternal ancestor. Familial pedigree showing the R274Q mutation in a patient with an open NTD, a mutation present in the mother (asterisk) but absent in the father, a case with a history of familial NTDs (mother and aunt have mild NTD vertebral schisis) represented by the cross-hatched circles. (B) Schematic representation of the secondary structure of GFP-tagged hVangl1 protein with the locations of mutants. The position of the HA tag located extracellularly at position 139 (used for surface expression and surface expression of Vangl protein) and of both mutants located intracellularly between TM1 and TM2. (C) Sequence conservation of mutations across species.

both substitutions. *VANGL1*<sup>R274Q</sup> was identified in a familial case of a NTD, where the proband is a 19-year-old female with an open NTD with both the mother (who is also a carrier) and aunt suffering from vertebral schisis, a milder NTD.<sup>2</sup> R274Q maps to the C-terminal intracellular domain of *VANGL2*, and the invariant arginine forms part of a putative D-box ubiquitination motif (RXXLXXD/E/X)<sup>3</sup> (Figure 1B,C). *VANGL1*<sup>R181Q</sup> was detected in an 8-year-old Italian male with myelomeningocele; the boy's mother also carries the R181Q mutation but is phenotypically normal, suggesting incomplete penetrance of the genetic effect (Figure 1A).<sup>28</sup> R181Q (and the corresponding R177H mutation in *VANGL2*) maps to the short 16-amino acid intracellular domain linking TM domains 2 and 3, which is the site of two additional disease-specific

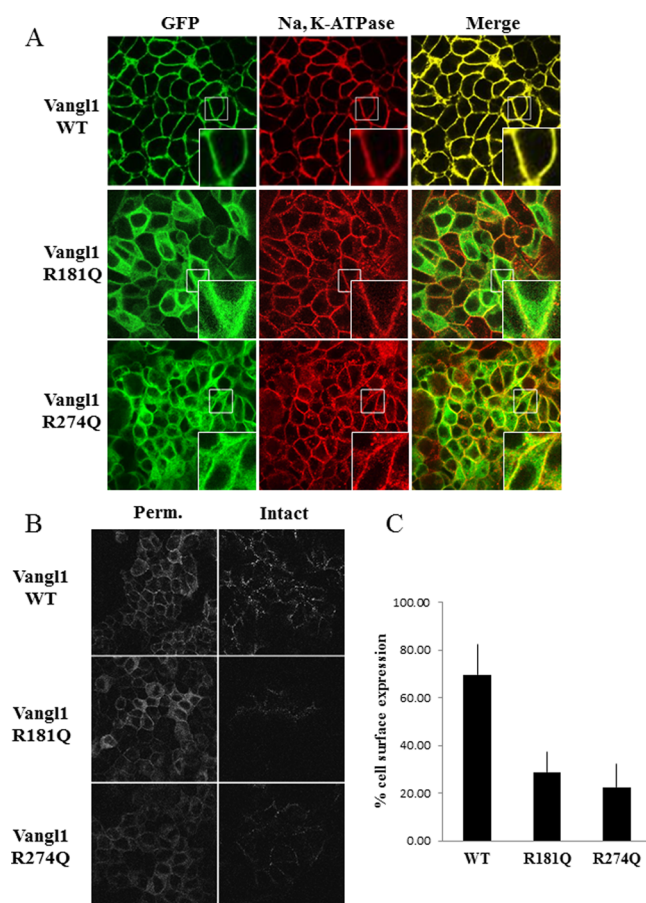


**Figure 2.** Cellular localization, surface expression, and quantification of WT, R181Q, and R274Q hVangl1 mutations in stably transfected MDCK cells. (A) Stably transfected MDCK cells expressing GFP-tagged hVangl1 WT, hVangl1 R181Q, or hVangl1 R274Q (green) were grown to confluency on coverslips, stained with plasma membrane marker Na,K-ATPase (red), and analyzed by confocal microscopy. The merged images show the WT protein colocalizing with Na,K-ATPase (yellow), while intracellular staining was observed for the R181Q and R274Q mutants. Images are representative of three independent experiments. (B) Cells expressing the three constructs (including an extracellular HA tag at position 139) were analyzed by confocal microscopy in either nonpermeabilized or permeabilized (0.5% Triton X-100) conditions followed by incubation with a mouse anti-HA antibody. Images are representative of at least three independent experiments. (C) Amount of surface expression quantified in a different experiment using the same cells (in either intact or permeabilized condition) by following incubation with the HA antibody with an HRP-coupled secondary antibody and colorimetrically quantifying an HRP substrate (OPD) by spectrometry. The amount of HA-tagged WT, R181Q, or R274Q protein expressed at the cell surface of MDCK cells (intact) was shown as a percentage of total protein expression (permeabilized condition).

mutations are detected only under permeabilized conditions, suggesting that both of these human mutations are not properly targeted to the plasma membrane. In addition, cell surface expression of the HA tag was further quantified by an ELISA using a secondary antibody coupled to horseradish peroxidase and applied to WT-, R181Q-, and R274Q-expressing cells under permeabilized (total) and nonpermeabilized (cell surface) conditions (Figure 2C). The amount of HA-bound antibody was quantified in stably expressing MDCK cells. In cells expressing the WT protein, 70% of the HA-Vangl1-

associated signal was at the cell surface and only 29% of R181Q and 22% of R274Q (Figure 2C). Taken together, these results suggest that the NTD-specific human Vangl1 mutations R181Q and R274Q interfered with proper plasma membrane targeting of the protein and reduced the level of cell surface expression.

#### Subcellular Localization of R181Q and R274Q VANGL1 Mutations in Stably Transfected MDCK Cells.

Subcellular localization of the R181Q and R274Q mutations was also investigated by confocal microscopy followed by examination of serial cell sections (Z-stacks). This analysis (Figure 3A) showed that the WT Vangl1 protein is expressed

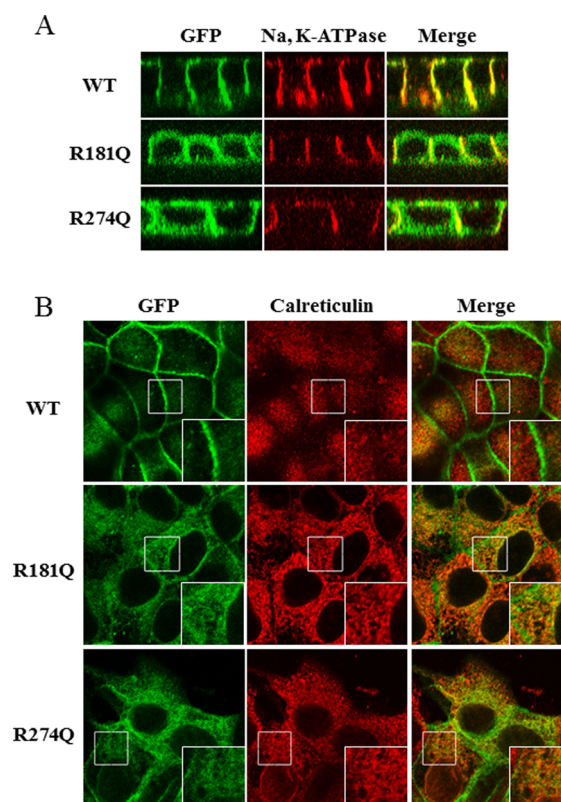


**Figure 3.** Subcellular localization of WT, R181Q, and R274Q hVangl1 in stably transfected MDCK cells. (A) Cells expressing GFP-tagged hVangl1 mutations (green) were grown to confluency, stained with Na,K-ATPase (red), and analyzed by Z-line image analysis on the confocal microscope. Representative X-Z sections are shown. The merged images show that both R181Q and R274Q localize to an intracellular compartment and do not colocalize with Na,K-ATPase (yellow). (B) Cells expressing GFP-tagged hVangl1 mutations (green) were grown to confluency and stained with ER marker calreticulin (red), and subcellular localization was analyzed by confocal microscopy. Merged images show that R181Q and R274Q mutants are trapped in the ER, colocalizing with calreticulin (yellow and boxed magnification), while the WT protein is expressed at the plasma membrane. Images are representative of three independent experiments.

predominantly in the lateral membrane of polarized MDCK cells, where it colocalizes with Na,K-ATPase. This localization is largely lost in the R181Q and R274Q mutants, which instead display a more diffuse intracellular staining associated with the periphery of the cells (Figure 3A). The altered plasma membrane recruitment and the more pronounced intracellular staining noted for R181Q and R274Q suggested these mutations may be targeted to an intracellular endomembrane

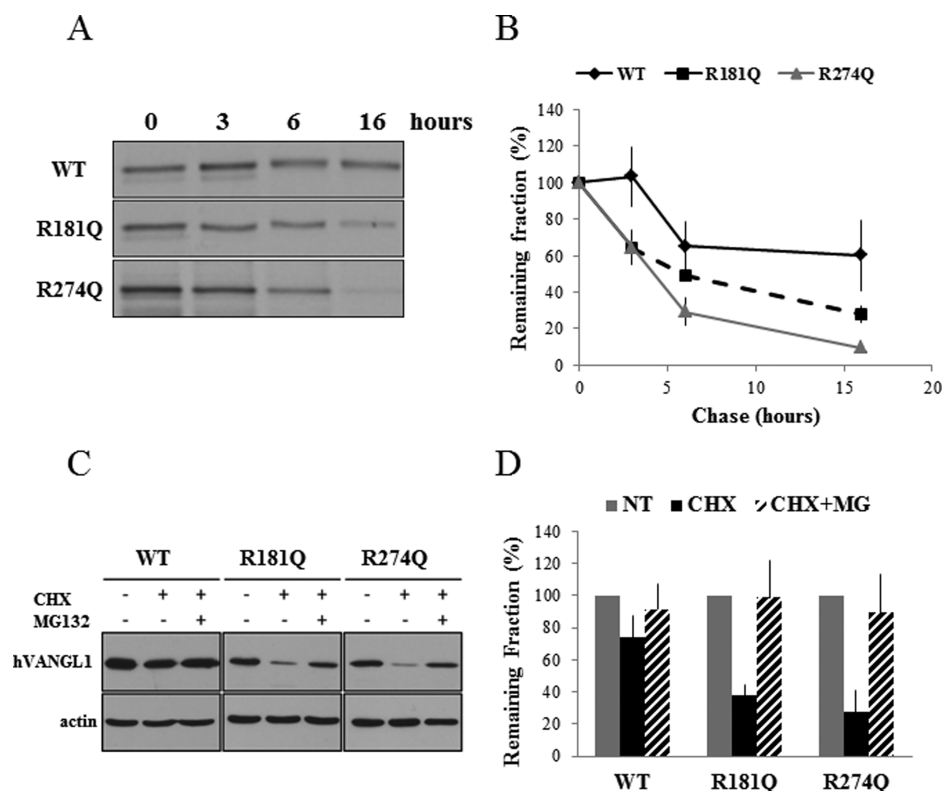


**Figure 4.** Cellular stability, half-life, and degradation studies of WT, R181Q, and R274Q hVangl1 in stably transfected MDCK cells. (A) Cells expressing a GFP-tagged hVangl1 mutation were metabolically labeled by a 60 min pulse of [ $^{35}$ S]Met/Cys, followed by incubation in a radioisotope-free medium, and chased for different periods of time (up to 16 h). Cells were lysed and immunoprecipitated, followed by gel electrophoresis and autoradiography. (B) Quantification of the remaining protein was conducted on the scans of the autoradiograms using ImageJ. The disappearance of the protein is shown as a fraction (percent) of the total protein at time  $T_0$ , which is set at 100%. The graph shows the mean of three experiments  $\pm$  the standard deviation. (C) Cells expressing GFP-tagged hVangl1 mutations were grown to confluence and treated with cycloheximide (20  $\mu$ g/mL) for 6 h in the presence or absence of proteasomal inhibitor MG-132 (5  $\mu$ g/mL). Cells were lysed, and 50  $\mu$ g of protein was separated by gel electrophoresis. Actin was used as an internal loading control. (D) Remaining fractions of WT, R181Q, and R274Q.

compartment (Figures 2A,B and 3A), possibly the endoplasmic reticulum (ER). Retention and accumulation of pathological *Lp*-associated mutations in the ER have been described previously<sup>21</sup> and caused by aberrant processing by Sec24b into COPII vesicles, for ER to Golgi transport.<sup>23,31</sup> Therefore, we investigated this possibility by double immunofluorescence with the ER marker calreticulin (Figure 3B). While WT Vangl1 does not colocalize with calreticulin (Figure 3B, top panel), the R181Q and R274Q mutations show overlapping staining with calreticulin [yellow-orange color in merged images (Figure 3B)]. These results indicate that, like *Lp*-specific pathological mutations causing NTD *in vivo*,<sup>4</sup> the human R181Q and R274Q mutations detected in familial cases of NTD show impaired plasma membrane targeting and appear to be retained in the ER.

**Stability of the R181Q and R274Q hVangl1 Mutations in Transfected MDCK Cells.** The retention of membrane protein mutations in the ER is frequently associated with decreased protein stability and an increased level of degradation.<sup>32</sup> The stability of the R181Q and R274Q mutations was investigated in pulse–chase studies, and the half-life of WT and mutant proteins was determined. Cells were metabolically labeled with [ $^{35}$ S]methionine/cysteine for 60 min, followed by a chase period in radioisotope-free medium (1–16 h), and cell extracts were analyzed by immunoprecipitation with an antibody directed against a c-Myc epitope tag inserted at the N-terminus of the proteins. A representative autoradio-

gram is shown in Figure 4A, while quantification of the average of several experiments was used to calculate half-lives of each protein (Figure 4B). These studies show that the half-life of WT Vangl1 in MDCK cells is  $\sim$ 16 h, as we have previously documented.<sup>21</sup> On the other hand, the half-lives of the R181Q and R274Q mutants were significantly shorter at  $\sim$ 7 and  $\sim$ 5 h, respectively (Figure 4B). The stability of the WT and mutants was also monitored in cells following inhibition of protein synthesis [cycloheximide (CHX)], and their possible degradation via the proteasome (MG-132) was also investigated (Figure 4C,D). CHX treatment of WT had an only modest effect on the level of protein, with an  $\sim$ 25% reduction in WT protein, compared to  $\sim$ 60 and  $\sim$ 70% reductions in R181Q and R274Q, respectively (Figure 4D). On the other hand, addition of MG-132 to CHX-treated cells resulted in a large increase in the level of detectable mutant protein expression, with a  $>$ 60% increase for both mutants compared to only a modest 17% increase for the WT protein, clearly indicating mutant proteins are degraded in a proteasomally dependent manner. These results suggest that R181Q and R274Q mutations are pathogenic; they prevent plasma membrane insertion and cause retention in the ER, which is associated with reduced protein stability and an increased level of degradation via the proteasome.



## DISCUSSION

Early studies in *Drosophila* identified a role for Van Gogh proteins (Vangl homologues) in providing planar cell polarity information to epithelial cells, including planar polarization of cellular appendages.<sup>17</sup> Subsequent studies in *Xenopus* demonstrated that Vangl and other PCP proteins are also required for convergent extension movements during tissue patterning, including formation of the neural tube.<sup>33</sup> Positional cloning of *Vangl2* as the gene mutated in the *Lp* mutant mice demonstrated that in mammals Vangl proteins were involved in both planar cell polarity (orientation of the stereociliary bundles of the neurosensory epithelium of the organ of Corti) and convergent extension movements (neurogenesis and cardiogenesis).<sup>4,7</sup> Subsequently, mutations in other PCP genes were found to similarly cause neural tube defects in mice: this includes homozygosity for loss-of-function alleles in *Celsr1*, *Dvl1/Dvl2*, *Dvl2/Dvl3*, *Fzd3/6*, *PTK7*, *Scribble*, *Ror2*, and *Sec24b*, as well as combined heterozygosity for mutations at *Vangl2*<sup>Lp/+</sup> and other PCP genes.<sup>4</sup> In humans, the study of familial and sporadic cases of NTDs identified unique, disease-associated mutations in *VANGL1*<sup>2,28,30</sup> and *VANGL2*<sup>27,29</sup> proteins, further highlighting a very important role for mammalian Vangl proteins in PCP signaling, CE movements, and particularly formation of the neural tube. The 20 mutations identified in human *VANGL1* and *VANGL2* in cohorts of familial or sporadic NTD cases have been flagged as pathological on the basis of the following criteria. (a) They are patient-specific and are not present in ethnically matched unaffected controls. (b) They affect residues that are highly conserved among Vangl homologues. (c) They represent nonconserved substitutions that are likely to affect local protein structure. (d) In some instances, they behave as loss-of-function mutations in complementation studies in model organisms such as yeast (interaction with Dvl family members)<sup>22,27</sup> and zebrafish (complementation of CE phenotypes induced by silencing of the fish *trilobite* ortholog).<sup>2,34</sup> However, the mechanistic basis for the impaired function of these human mutations has not yet been investigated.

To start to characterize the biochemical basis of altered function in Vangl mutations found in human NTD patients, we elected to study the R181 and R274 residues. R181 and R274 are independently mutated to glutamine in *VANGL1* (R181Q and R274Q) in two unrelated NTD patients and mutated to histidine in *VANGL2* (R177H and R270H) at the homologous position in two other unrelated NTD patients. In addition, both R181 and R274 are extremely conserved in the *VANGL* family, R274 being invariant and R181 being highly conserved, with both mapping to protein subdomains that also show a high degree of sequence conservation (Figure 1). Finally, the charged positive side chain of arginine is lost in both substitutions found in independent NTD patients. Together, these findings suggested that R181 and R274 play critical and conserved structural and functional roles in Vangl protein functions, and are particularly mutation-sensitive, and that the loss of either of these arginines results in altered function. Hence, we compared the biochemical features of R181Q and R274Q to those of the WT Vangl1 protein following expression of each mutation (reconstructed in the Vangl1 protein template) in MDCK epithelial kidney cells. Our results indicate that normal membrane targeting of these two mutations is impaired, and rather than being recruited to the plasma membrane (colocalization with Na,K-ATPase at the basolateral

side of polarized epithelial cells), R181Q and R274Q are found in an intracellular endomembrane compartment that shows overlap staining with the ER marker calreticulin. The two mutations show reduced stability and 2- and 4-fold reductions in protein half-life, respectively, in MDCK cells (>20 h for WT, ~9 h for R181Q, and ~5 h for R274Q). Compared to WT, both mutants were found to be rapidly degraded in a proteasome-dependent and MG-132-sensitive fashion. The behavior of the two human mutations is essentially identical to what we have recently demonstrated for the three available *Vangl2* alleles associated with the severe neural tube defect in the *Lp* mouse, i.e., D255E (*Lp*<sup>m1Jus</sup>), R259L (*Lp*<sup>m2Jus</sup>), and S464N (*Lp*).<sup>20,21</sup> The effect of the R181Q and R274Q mutations on membrane targeting and protein stability is specific and is not seen in other *VANGL1* and *VANGL2* mutants associated with neural tube defects. For example, an L202F mutation was identified in a 9-year-old female of Italian origin with an open NTD (myelomeningocele). This mutant maps to the “WLF” motif that is invariant in the *VANGL* protein family. The L202F mutant is properly targeted to the plasma membrane and is not retained intracellularly, in contrast to the R181Q and R274Q mutations (Figure 1 of the Supporting Information). The mechanistic basis for the loss of function in L202F remains to be established but may involve the impairment of interaction with *VANGL* binding partners such as members of the DVL protein family. Together, these findings clearly establish that the human R181Q and R274Q mutations detected in familial cases of NTD (a) have impaired function, (b) are phenotypically indistinguishable from the S464N allele characteristic of the *Lp* mutation, and (c) are likely pathological *in vivo*, contributing to the etiology of NTDs in these patients. By the same token, it is very likely that the R177H and R270H substitutions detected in NTD cohorts at the homologous positions of human *VANGL2* are also pathological. Finally, our findings provide a set of simple biochemical assays *in vitro* in which the impact of the *VANGL1* and *VANGL2* mutations detected in clinical specimens on protein function can be formally assessed.

It is important to note that the *VANGL1*<sup>R181Q</sup>, *VANGL1*<sup>R274Q</sup>, *VANGL2*<sup>R177H</sup>, and *VANGL2*<sup>R270H</sup> mutations have been detected as heterozygous mutations in clinical cases of NTDs.<sup>2,28,29</sup> This suggests that these allelic mutations at *VANGL1* and *VANGL2* behave either as haploid-insufficient in a gene-dosage-dependent pathway or as partially penetrant with negative codominance. This situation is very similar to the current debate regarding the mode of inheritance of pathological *Lp*-associated *Vangl* mutations in mice, which have also been alternatively assigned as dominant negative or loss of function in gene-dosage-dependent pathways.<sup>4</sup> Favoring a dominant negative effect are the observations in mice that (a) several *Vangl2*-associated PCP phenotypes appear to be more severe for *Lp* alleles (*Vangl2*<sup>D255E</sup> and *Vangl2*<sup>S464N</sup>) than for a null allele<sup>14</sup> and (b) *Vangl1* and *Vangl2* appear to physically interact and, in cotransfection experiments, *Lp* alleles disrupt *Vangl1*–*Vangl2* interactions, as well as trafficking and membrane targeting of *Vangl1* and *Vangl2*,<sup>14</sup> and decrease the level of post-translational modification of the WT protein.<sup>26,35</sup> Favoring haploid insufficiency in a gene-dosage-dependent pathway are the reports that (a) experimental overexpression or silencing of core PCP genes causes the same phenotype in different animal models tested, (b) all experimentally induced or naturally occurring *Vangl2* mutations described so far show varying degrees of the same phenotype in

mice (looped tail, inner ear defects) in heterozygotes and homozygotes *in vivo*,<sup>4</sup> (c) *Lp*-associated Vangl2 protein mutations are expressed at lower levels *in vivo* and display reduced stabilities and shorter half-lives when tested *in vitro*,<sup>7,10,11</sup> and (d) colocalization studies by double immunofluorescence and confocal microscopy in transfected MDCK cells show that expression of Vangl2<sup>D255E</sup> has no effect on membrane targeting of WT Vangl2.<sup>21</sup>

In conclusion, our findings identify R181 and R274 as critical arginines that are essential for the normal function of Vangl proteins. Their independent substitution with glutamine or histidine in multiple independent patients with NTDs causes a biochemical phenotype that is indistinguishable from those of known mutations in Vangl2 that are associated with NTD *in vivo* in the *Lp* mouse. Hence, our study strongly suggests that R181Q and R274Q in *VANGL1* are pathological and cause neural tube defects in humans.

## ■ ASSOCIATED CONTENT

### ■ Supporting Information

Schematic representation, multiple-sequence alignment, and cellular localization of the L202F variant (Figure 1). This material is available free of charge via the Internet at <http://pubs.acs.org>.

## ■ AUTHOR INFORMATION

### Corresponding Author

\*Department of Biochemistry and Complex Traits Program, McGill University, 3549 Drummond, Room 366, Montreal, QC, Canada H3G-0B1. E-mail: [philippe.gros@mcgill.ca](mailto:philippe.gros@mcgill.ca).

### Notes

The authors declare no competing financial interest.

## ■ ACKNOWLEDGMENTS

Image acquisition, data analysis, and image processing were conducted on equipment and with the assistance of the McGill Life Science Complex Imaging Facility, which was funded by the Canadian Foundation for Innovation.

## ■ REFERENCES

- (1) Greene, N. D., Stanier, P., and Copp, A. J. (2009) Genetics of human neural tube defects. *Hum. Mol. Genet.* 18, R113–R129.
- (2) Kibar, Z., Torban, E., McDermid, J. R., Reynolds, A., Berghout, J., Mathieu, M., Kirillova, I., De Marco, P., Merello, E., Hayes, J. M., Wallingford, J. B., Drapeau, P., Capra, V., and Gros, P. (2007) Mutations in *VANGL1* associated with neural-tube defects. *N. Engl. J. Med.* 356, 1432–1437.
- (3) Choi, E., Dial, J. M., Jeong, D. E., and Hall, M. C. (2008) Unique D box and KEN box sequences limit ubiquitination of Acm1 and promote pseudosubstrate inhibition of the anaphase-promoting complex. *J. Biol. Chem.* 283, 23701–23710.
- (4) Torban, E., Iliescu, A., and Gros, P. (2012) An expanding role of Vangl proteins in embryonic development. *Curr. Top. Dev. Biol.* 101, 237–261.
- (5) Bassuk, A. G., and Kibar, Z. (2009) Genetic basis of neural tube defects. *Seminars in Pediatric Neurology.* 16, 101–110.
- (6) Juriloff, D. M., and Harris, M. J. (2012) A consideration of the evidence that genetic defects in planar cell polarity contribute to the etiology of human neural tube defects. *Birth Defects Res., Part A* 94, 824–840.
- (7) Kibar, Z., Vogan, K. J., Groulx, N., Justice, M. J., Underhill, D. A., and Gros, P. (2001) *Ltap*, a mammalian homolog of *Drosophila* Strabismus/*Van Gogh*, is altered in the mouse neural tube mutant Loop-tail. *Nat. Genet.* 28, 251–255.
- (8) Murdoch, J. N., Doudney, K., Paternotte, C., Copp, A. J., and Stanier, P. (2001) Severe neural tube defects in the loop-tail mouse result from mutation of *Lpp1*, a novel gene involved in floor plate specification. *Hum. Mol. Genet.* 10, 2593–2601.
- (9) Kibar, Z., Gauthier, S., Lee, S. H., Vidal, S., and Gros, P. (2003) Rescue of the neural tube defect of loop-tail mice by a BAC clone containing the *Ltap* gene. *Genomics* 82, 397–400.
- (10) Kibar, Z., Underhill, D. A., Canonne-Hergaux, F., Gauthier, S., Justice, M. J., and Gros, P. (2001) Identification of a new chemically induced allele (*Lp(m1Jus)*) at the loop-tail locus: Morphology, histology, and genetic mapping. *Genomics* 72, 331–337.
- (11) Guyot, M. C., Bosoi, C. M., Kharfallah, F., Reynolds, A., Drapeau, P., Justice, M., Gros, P., and Kibar, Z. (2011) A novel hypomorphic *Looptail* allele at the planar cell polarity Vangl2 gene. *Dev. Dyn.* 240, 839–849.
- (12) Torban, E., Wang, H. J., Patenaude, A. M., Riccomagno, M., Daniels, E., Epstein, D., and Gros, P. (2007) Tissue, cellular and sub-cellular localization of the Vangl2 protein during embryonic development: Effect of the *Lp* mutation. *Gene Expression Patterns* 7, 346–354.
- (13) Torban, E., Patenaude, A. M., Leclerc, S., Rakowiecki, S., Gauthier, S., Andelfinger, G., Epstein, D. J., and Gros, P. (2008) Genetic interaction between members of the Vangl family causes neural tube defects in mice. *Proc. Natl. Acad. Sci. U.S.A.* 105, 3449–3454.
- (14) Yin, H., Copley, C. O., Goodrich, L. V., and Deans, M. R. (2012) Comparison of phenotypes between different vangl2 mutants demonstrates dominant effects of the *Looptail* mutation during hair cell development. *PLoS One* 7, e31988.
- (15) Fanto, M., and McNeill, H. (2004) Planar polarity from flies to vertebrates. *J. Cell Sci.* 117, 527–533.
- (16) Klein, T. J., and Mlodzik, M. (2005) Planar cell polarization: An emerging model points in the right direction. *Annu. Rev. Cell Dev. Biol.* 21, 155–176.
- (17) McNeill, H. (2010) Planar cell polarity: Keeping hairs straight is not so simple. *Cold Spring Harbor Perspect. Biol.* 2, a003376.
- (18) Strutt, D. I. (2002) The asymmetric subcellular localisation of components of the planar polarity pathway. *Semin. Cell Dev. Biol.* 13, 225–231.
- (19) Wallingford, J. B., Fraser, S. E., and Harland, R. M. (2002) Convergent extension: The molecular control of polarized cell movement during embryonic development. *Dev. Cell* 2, 695–706.
- (20) Iliescu, A., Gravel, M., Horth, C., Kibar, Z., and Gros, P. (2011) Loss of membrane targeting of Vangl proteins causes neural tube defects. *Biochemistry* 50, 795–804.
- (21) Gravel, M., Iliescu, A., Horth, C., Apuzzo, S., and Gros, P. (2010) Molecular and cellular mechanisms underlying neural tube defects in the loop-tail mutant mouse. *Biochemistry* 49, 3445–3455.
- (22) Torban, E., Wang, H. J., Groulx, N., and Gros, P. (2004) Independent mutations in mouse Vangl2 that cause neural tube defects in looptail mice impair interaction with members of the Dishevelled family. *J. Biol. Chem.* 279, 52703–52713.
- (23) Wansleben, C., Feitsma, H., Montcouquiol, M., Kroon, C., Cuppen, E., and Meijlink, F. (2010) Planar cell polarity defects and defective Vangl2 trafficking in mutants for the COPII gene *Sec24b*. *Development* 137, 1067–1073.
- (24) Guo, Y., Zanetti, G., and Schekman, R. (2013) A novel GTP-binding protein-adaptor protein complex responsible for export of Vangl2 from the trans Golgi network. *Elife* 2, e00160.
- (25) Kalabis, J., Rosenberg, I., and Podolsky, D. K. (2006) Vangl1 protein acts as a downstream effector of intestinal trefoil factor (ITF)/TFF3 signaling and regulates wound healing of intestinal epithelium. *J. Biol. Chem.* 281, 6434–6441.
- (26) Gao, B., Song, H., Bishop, K., Elliot, G., Garrett, L., English, M. A., Andre, P., Robinson, J., Sood, R., Minami, Y., Economides, A. N., and Yang, Y. (2011) Wnt signaling gradients establish planar cell polarity by inducing Vangl2 phosphorylation through Ror2. *Dev. Cell* 20, 163–176.



- (27) Lei, Y. P., Zhang, T., Li, H., Wu, B. L., Jin, L., and Wang, H. Y. (2010) VANGL2 mutations in human cranial neural-tube defects. *N. Engl. J. Med.* 362, 2232–2235.
- (28) Kibar, Z., Bosoi, C. M., Kooistra, M., Salem, S., Finnell, R. H., De Marco, P., Merello, E., Bassuk, A. G., Capra, V., and Gros, P. (2009) Novel mutations in VANGL1 in neural tube defects. *Hum. Mutat.* 30, E706–E715.
- (29) Kibar, Z., Salem, S., Bosoi, C. M., Pauwels, E., De Marco, P., Merello, E., Bassuk, A. G., Capra, V., and Gros, P. (2011) Contribution of VANGL2 mutations to isolated neural tube defects. *Clin. Genet.* 80, 76–82.
- (30) Bartsch, O., Kirmes, I., Thiede, A., Lechno, S., Gocan, H., Florian, I. S., Haaf, T., Zechner, U., Sabova, L., and Horn, F. (2012) Novel VANGL1 Gene Mutations in 144 Slovakian, Romanian and German Patients with Neural Tube Defects. *Mol. Syndromol.* 3, 76–81.
- (31) Merte, J., Jensen, D., Wright, K., Sarsfield, S., Wang, Y., Schekman, R., and Ginty, D. D. (2010) Sec24b selectively sorts Vangl2 to regulate planar cell polarity during neural tube closure. *Nat. Cell Biol.* 12, 41–46 (suppl. pp 41–48).
- (32) Ellgaard, L., and Helenius, A. (2003) Quality control in the endoplasmic reticulum. *Nat. Rev. Mol. Cell Biol.* 4, 181–191.
- (33) Darken, R. S., Scola, A. M., Rakeman, A. S., Das, G., Mlodzik, M., and Wilson, P. A. (2002) The planar polarity gene strabismus regulates convergent extension movements in *Xenopus*. *EMBO J.* 21, 976–985.
- (34) Reynolds, A., McDearmid, J. R., Lachance, S., De Marco, P., Merello, E., Capra, V., Gros, P., Drapeau, P., and Kibar, Z. (2010) VANGL1 rare variants associated with neural tube defects affect convergent extension in zebrafish. *Mech. Dev.* 127, 385–392.
- (35) Song, H., Hu, J., Chen, W., Elliott, G., Andre, P., Gao, B., and Yang, Y. (2010) Planar cell polarity breaks bilateral symmetry by controlling ciliary positioning. *Nature* 466, 378–382.